

Design of high gain broadband microstrip patch antenna for UWB/X/Ku band applications

Tapas Tewary^a, Smarajit Maity^a, Surajit Mukherjee^b, Avisankar Roy^b, Partha Pratim Sarkar^c, Sunandan Bhunia^{d,*}

^a Academy of Technology, G.T.Road (Adisaptagram), Aedconagar, Hooghly, West Bengal, India

^b Haldia Institute of Technology, Haldia, West Bengal, India

^c University of Kalyani, West Bengal, India

^d Central Institute of Technology, Kokrajhar, Assam, India

ARTICLE INFO

Keywords:

Broadband

Compact

Frequency selective surface

High gain

Microstrip patch antenna

ABSTRACT

A miniature ($20 \text{ mm} \times 14 \text{ mm} \times 1.6 \text{ mm}$) microstrip line fed broadband antenna with high gain is proposed in this research work. The proposed antenna exhibits -10 dB impedance bandwidth of 19.5 GHz (5 GHz - 24.5 GHz) with a fractional bandwidth of 132% which covers major portion of UWB band (3.1 GHz - 10.6 GHz), X band (8 GHz - 12 GHz), Ku band (12 GHz - 18 GHz) and large part of K band (18 GHz - 27 GHz). A single layer frequency selective surface (FSS) is integrated with the proposed antenna to enhance the gain of 5.9 dBi over the entire frequency band. 6×6 FSS layer ($52.8 \text{ mm} \times 52.8 \text{ mm} \times 1.6 \text{ mm}$) is kept below the proposed antenna at suitable distance without hampering the reflection coefficient and flat gain characteristics of the antenna. Proposed antenna and FSS structure are designed and simulated by using CST Microwave Studio simulator and both are built on FR-4 substrate of 1.6 mm thickness with relative dielectric constant (ϵ_r) of 4.4 , loss tangent ($\tan\delta$) of 0.02 . The overall dimension of the proposed FSS integrated antenna is $52.8 \text{ mm} \times 52.8 \text{ mm} \times 21.2 \text{ mm}$, which is highly relevant for high-gain applications. Simulated results are validated experimentally by standard Microwave Test bench.

1. Introduction

Modern day communication technology challenges the researchers to design compact broadband antenna which can support multiple operating band at the same time. Earlier multiple antennas were designed to support multiple frequency bands in many devices which required huge space. Also system complexity increases with new frequency band up gradation. In current situation high bandwidth is necessary for high data rate wireless communication as well as for high accuracy radar application, satellite navigation system etc. These requirements can be fulfilled by designing broadband antenna. Microstrip patch antenna has been always a perfect solution due to its various advantages like low cost, light weight, low volume, easy integratability with existing system etc. But it suffers from narrow bandwidth and low gain. For this reason researchers are trying different approaches to achieve compact broadband high gain antenna with multiple resonant frequencies for application in multiple frequency bands. This includes use of different feeding methods, modified ground structure, parasitic

patch, slot loading in patch and ground, metamaterial, shorting pin, and dielectric substrate [1-2]. Impedance matching modified feed structure has been reported to achieve broadband nature effectively without disturbing major performance characteristics [3-4]. Another popular technique to enhance bandwidth is to use monopole structure along with modified feed structure, defective ground structure, slot loading in patch etc. [5-8]. Impedance bandwidth of a rectangular microstrip patch antenna has been increased significantly by using epsilon-near-zero (ENZ) material and reported in [9]. In addition to large bandwidth many applications require high gain antenna with stable radiation pattern. Also maximum radiation intensity in broadside direction is always desirable than omnidirectional radiation pattern. Optimization of patch and ground parameters has always been an effective way to achieve high gain [10-13]. At present using of frequency selective surface is a popular technique to improve gain and directivity of the antenna. Significant gain improvement is done by placing a single layer FSS or dual layer FSS below the antenna at suitable distance [14-19].

In this work, a miniaturized ($14 \text{ mm} \times 20 \text{ mm}$) broadband microstrip

* Corresponding author.

E-mail addresses: tapas.tewary@aot.edu.in (T. Tewary), smarajit.maity@aot.edu.in (S. Maity), bhuniasunandan@gmail.com (S. Bhunia).

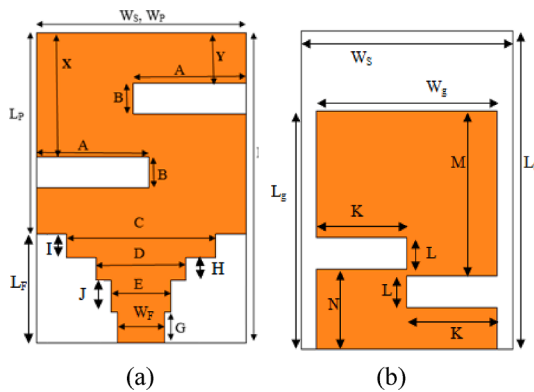


Fig. 1. Structure of (a) radiating patch and (b) ground plane of the proposed antenna.

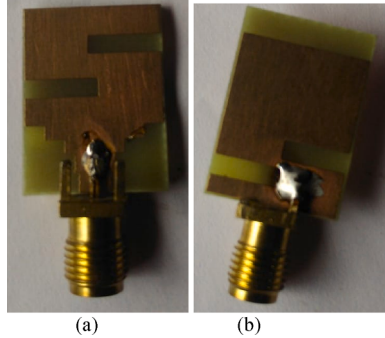


Fig. 2. Fabricated antenna (a) Radiating patch (b) Ground plane.

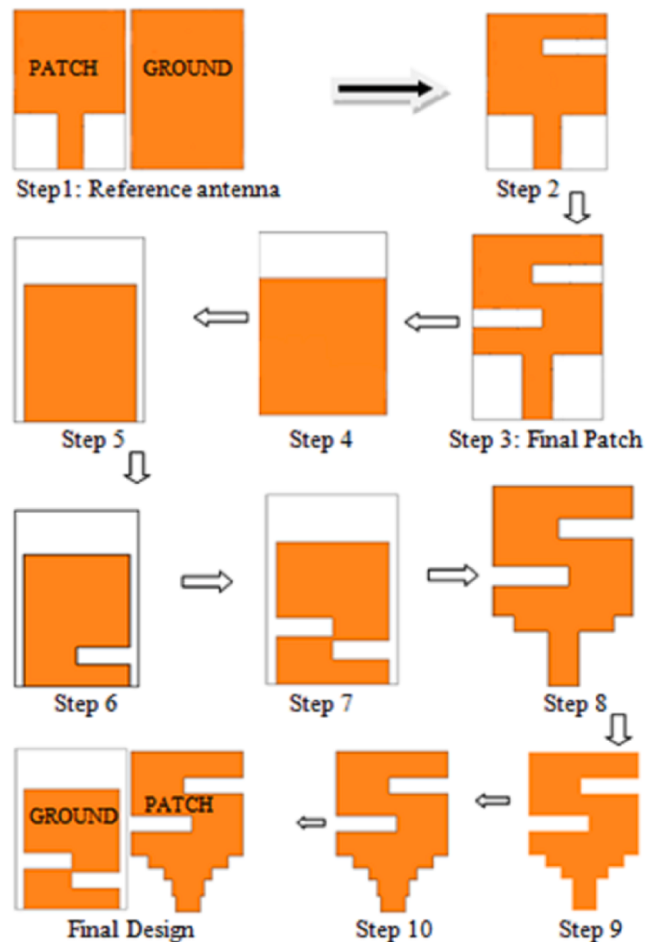


Fig. 3. Design steps of the proposed antenna.

Table 1
Antenna and FSS unit cell design parameter specification and dimensions (mm).

Parameters	Values	Parameters	Values	Parameters	Values
L_S	20	C	10	N	5
W_S, W_P	14	D	6	W_{FSS}	8.8
L_g	15	E	4	L_{FSS}	8.8
W_g	12	G, J	2	P	1.6
h (antenna)	1.6	H, I	1.5	Q	0.7
L_p	13	X	8	R	1.3
L_F	7	Y	3.25	S	3.6
W_F	3.1	K	6	g	0.1
A	7.5	L	2	h (FSS)	1.6
B	2	M	10.4		

patch antenna is designed, simulated, manufactured and verified experimentally. Broadband characteristics is achieved by incorporating slots in radiating patch, incorporating slots in reduced ground plane and by applying matching three step staircase structure in the feedline of the proposed antenna for better impedance matching. The proposed antenna exhibits a large impedance bandwidth of 19.5 GHz (5 GHz-24.5 GHz) with a fractional bandwidth of 132%. Measured peak gain of 3.06 dBi is achieved at 11.75 GHz. To enhance the overall antenna gain further a proposed single layer frequency selective surface (FSS) is placed below the antenna at optimum distance (18 mm). The composite structure of antenna with 6×6 FSS enhances the peak gain to 8.8 dBi with maximum gain enhancement of 5.9 dBi keeping the entire -10 dB impedance bandwidth unaltered. The antenna can be used to operate in UWB band, X band, Ku band, K band.

2. Design of antenna

The proposed antenna has been designed and simulated using CST

Table 2
Results of all design steps.

DesignSteps	-10 dB impedance BW(GHz)	Peak gain(dBi)
1	11.2-11.9, 19.6-20.35, 23.8-25...	4.06
2	9.3-10.9, 14.6-15.4, 19.77-25...	3.35
3	9.2-10.82, 11.85-12.5, 13.5-14.45, 16.75-25...	3.05
4	9.5-10.8, 12.6-13.2, 16.2-19.2, 19.9-25...	3.38
5	9.37-10, 10.9-11.66, 12.65-13.53, 15.65-25	3.20
6	11-11.66, 12.5-19.35, 22.9-25	3.52
7	8.9-10, 11-11.7, 12.7-19.4, 21-25...	2.93
8	7.25-11.6, 12.7-15.6, 16.6-19.6, 20.8-25...	3
9	6-25...	3.18
10	5-24.5	3.06

Microwave Studio Software. To design the antenna initially an FR4 substrate of dimension $L_S \times W_S \times h$ is taken. The radiating plane looks like 'S' on top of the substrate. Two identical rectangular slots, each of dimension $A \times B$ have been removed from the rectangular patch of dimension $L_p \times W_p$ to obtain 'S' shape radiating patch. The antenna is fed by a micro-strip line of staircase like structure. Initially a rectangular ground plane of dimension $L_g \times W_g$ is taken. Later the ground plane is modified to $L_g \times W_g$. The ground plane has been modified further by removing two identical rectangular slots each of dimension $K \times L$. Finally the feed line has been modified to a staircase like structure in order to achieve the broadband characteristics keeping the impedance near 50Ω [20]. The detailed geometry of radiating plane and ground plane are illustrated in Fig. 1 and the photograph of fabricated antenna is shown in Fig. 2. Table 1 illustrates the optimum design parameters of the proposed antenna.

Table 3

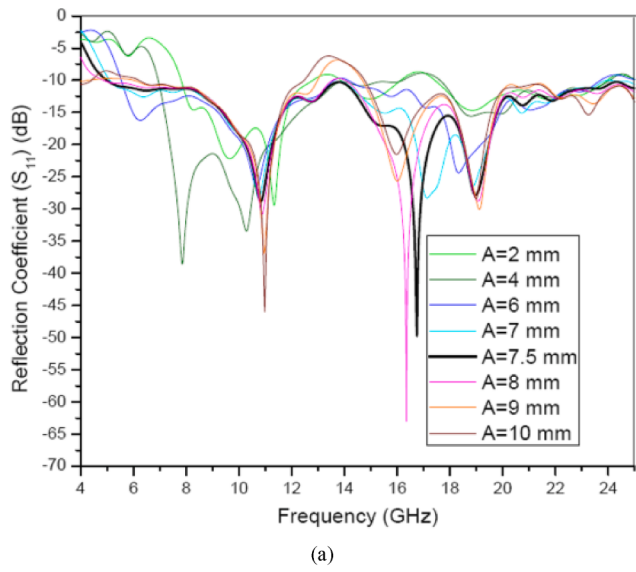
Variation of antenna characteristics with 'A' where $B = 2$ mm, $X = 8$ mm and $Y = 3.25$ mm.

A (mm)	-10 dB impedance B.W. (GHz)	Peak Gain(dBi)	A (mm)	-10 dB impedance B.W. (GHz)	Peak Gain(dBi)
2	7.8–12.7, 13.9–16.1, 17.4–23.9	3.04	7.5	5–24.5	3.06
4	6.94–16.17, 17.62–24,	3.72	8	4.86–13.53, 14–25	3.05
6	5.55–13.57, 14.14–23.69,	3.21	9	6–12.96, 14.68–25	3.45
7	5.11–23.9	3.03	10	6.2–12.46, 14.77–25	3.62

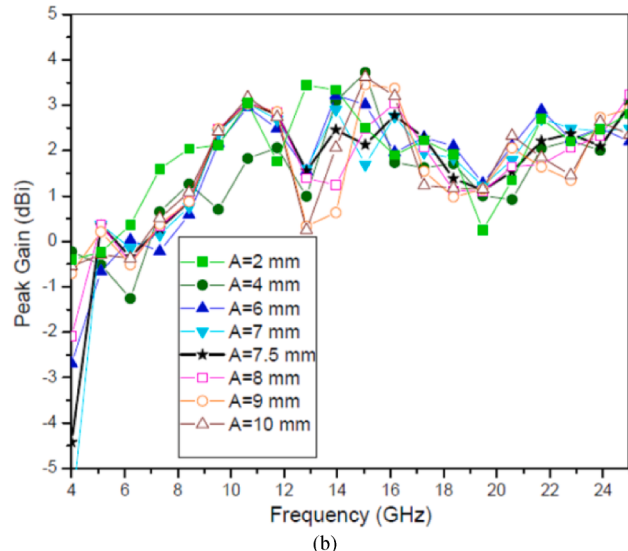
Table 4

Variation of antenna characteristics with 'B' where $A = 7.5$ mm, $X = 8$ mm and $Y = 3.25$ mm.

B (mm)	-10 dB impedance B. W. (GHz)	Peak Gain (dBi)	B (mm)	-10 dB impedance B.W. (GHz)	Peak Gain (dBi)
0.5	6.77–14.45, 16–19.56,	4.38	2	5–24.5	3.06
1	6.5–15, 15.7–19.5	4.24	2.5	4.44–6.9, 9.33–13.15, 14.35–25	3.02
1.5	6.4–19.4,	3.67	3	7–7.35, 15–20.84	2.21
1.75	6.33–19.43,	3.51	4	4.1–6.2	2.64

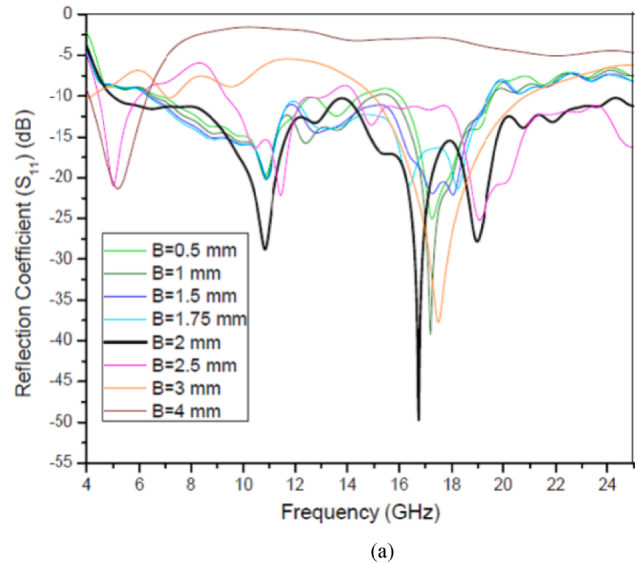


(a)

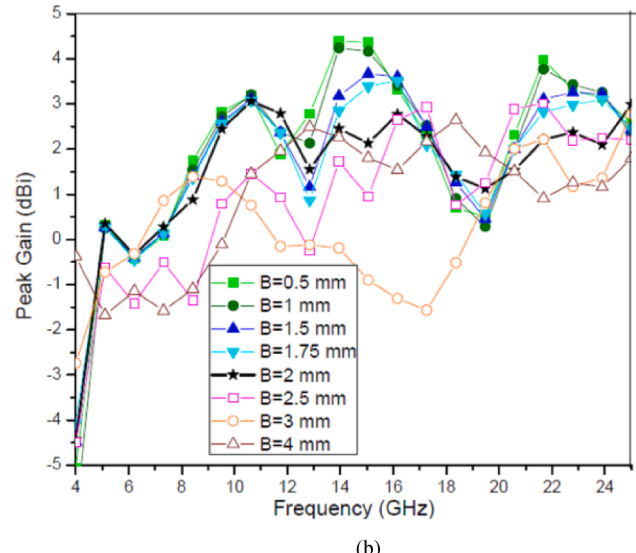


(b)

Fig. 4. (a) Reflection coefficient and (b) peak gain from Table 3.



(a)



(b)

Fig. 5. (a) Reflection coefficient and (b) peak gain from Table 4.

3. Design steps of proposed antenna

The reference antenna comprises of a rectangular patch of dimension $13 \times 14 \text{ mm}^2$ on top of the substrate of dimension $20 \times 14 \text{ mm}^2$ along with the same ground dimension as shown in step 1 in Fig. 3. The design summary of the proposed antenna has been illustrated from step 2 to step 10 as shown in the Fig. 3. This includes slot loading in patch (step 2 and step 3), modifying ground structure (step 4-step 7) and modifying feed structure (step 8-step 10). Slots in the patch disturb the current distribution as well as the current lines path resulting new resonant frequencies. In order to obtain wideband, the slots in the patch and ground are suitably placed so that the resonant frequencies are very

Table 5

Variation of antenna characteristics with 'X' where A = 7.5 mm, B = 2 mm and Y = 3.25 mm.

X (mm)	-10 dB impedance B.W. (GHz)	Peak Gain (dBi)	X (mm)	-10 dB impedance B.W. (GHz)	Peak Gain (dBi)
6	4.2–5.5, 6–6.5, 8.4–13.4, 14.35–20, 21.4–23.4	3.45	8	5–24.5	3.06
6.5	4.3–6.7, 8.3–20.6, 21.1–24,	3.79	8.5	5.13–13.76	2.69
7	4.5–7.65, 8.14–24.1, 24.7–24.9	4.15	9	5.32–21, 21.4–24.93	2.81
7.5	4.17–24.17	4.13	9.5	5.3–16, 17–20.75, 22.75–24.5	2.88

Table 6

Variation of antenna characteristics with 'Y' where A = 7.5 mm, B = 2 mm and X = 8 mm.

Y (mm)	-10 dB impedance B.W. (GHz)	Peak Gain (dBi)	Y (mm)	-10 dB impedance B. W. (GHz)	Peak Gain (dBi)
2	4.63–5.8, 9–11.8, 14.66–25	3.12	3.25	5–24.5	3.06
2.25	4.58–5.8, 9–11.9, 14.66–25	2.85	3.5	4.94–24.5	3.12
2.5	5.1–13.36, 13.95–24.24	3.12	4	5.13–24.4	3.14
3	5–24.5,	3.06	4.5	5.93–21.26	3.86

close to each other resulting a wider bandwidth due to the staggering effect. From the given data in Table 2 staggering effects for slot insertion in patch and ground with modified feed structure are observed. This staggering effects help to achieve broadband (5 GHz-24.5 GHz) operation.

4. Parametric analysis

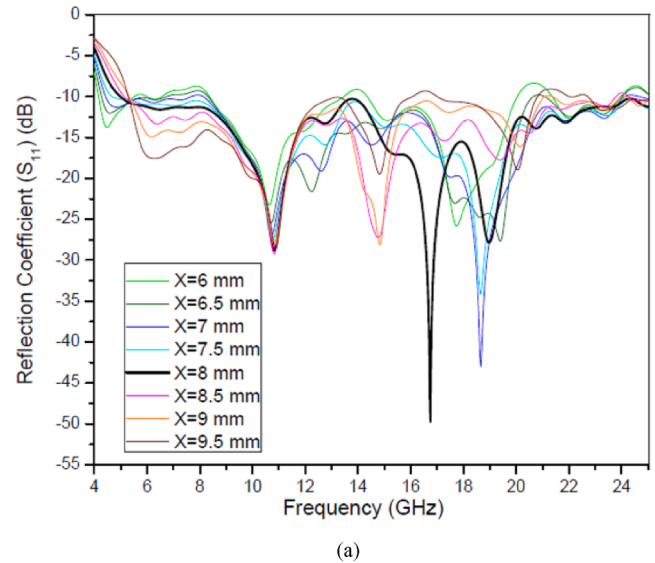
Rigorous parametric analysis has been performed to find out the effect of dominant parameters of proposed antenna on reflection characteristics and gain characteristics. The performance of antenna with variation of slot length, slot width on radiating patch, ground plane are analyzed and also impedance matching modified feed structure is studied to finalize the optimum dimension of each parameter. The detail parametric analysis is carried out by varying one parameter at a time while all other parameters are kept at constant. Tables 3 and 4 and Figs. 4–5 illustrate how the two slots (each of dimension A × B) on radiating patch affect reflection and gain characteristics. Slot length (A) is varied from 2 mm to 10 mm and slot width (B) is varied from 0.4 mm to 4 mm. It can be observed that wideband characteristics can be achieved by bringing multiple bands close to each other and merge them together for optimum values of A, B. The distance of the left slot from top edge of the patch (X) is varied from 6 mm to 9.5 mm and distance of the right slot from the top edge of the patch(Y) is varied from 2 mm to 4.5 mm. From the simulation results shown in Tables 5 and 6 and Figs. 6–7 proper positions (X and Y) of slots are finalized.

Both from Table 3 and Fig. 4, it is observed that broadband characteristic is achieved for A = 7.5 mm.

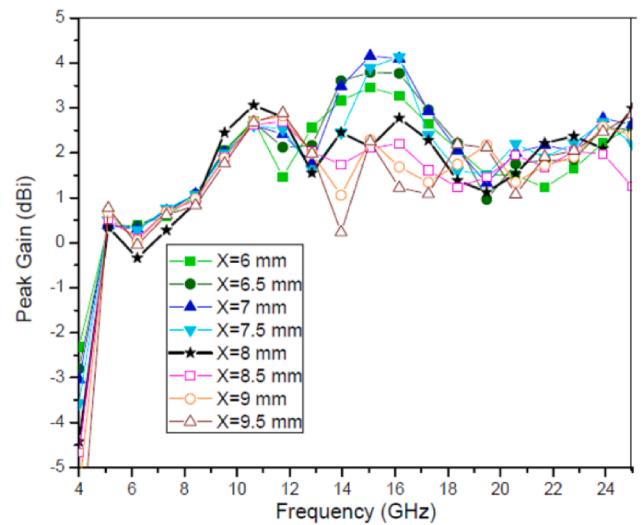
Both from Table 4 and Fig. 5, it is noticed that broadband characteristic is achieved for B = 2 mm.

Both from Table 5 and Fig. 6, it is observed that broadband characteristic is achieved for X = 8 mm.

Both from Table 6 and Fig. 7, it is clear that broadband operation is achieved for Y = 3.25 mm. Effect of ground plane modification is illustrated in Tables 7–11 and corresponding graphs are shown in Figs. 8–12. These includes reduction of ground plane length (L_g), ground plane width (W_g) and incorporation of two slots (each of dimension K × L) at proper positions (M, N) on reduced ground plane. Effect of ground plane length (L_g) variation is obtained by varying the distance of the right slot



(a)



(b)

Fig. 6. (a) Reflection coefficient and (b) peak gain from Table 5.

from the top edge of the ground (M) and is shown in Table 7 and Fig. 8. 'M' is varied from 3 mm to 12 mm and it can be observed that for optimum value of 'M' multiple bands merge together to provide wideband characteristics. Tables 8 and 9 and Figs. 9–10 illustrates the effect of ground plane slot length and width optimization. The ideal positions of two slots on the ground plane are finalized by varying the distance of the slots (M, N) from top edge of the ground plane. Table 11 and Fig. 12 shows the effect of variation of ground plane width (W_g) when 'Wg' is varied from 10.5 mm to 14 mm. The optimum value is finalized at 12 mm when the proposed antenna exhibits wideband characteristics. Modified ground plane helps to achieve a purely resistive input impedance to obtain broadband characteristics.

Both from Table 7 and Fig. 8, it is observed that for M = 10.4 mm broadband characteristic is obtained.

Both from Table 8 and Fig. 9, it is cleared that broadband characteristic is achieved for L = 2 mm.

Both from Table 9 and Fig. 10, it is observed that for K = 6 mm broadband characteristic is obtained.

Both from Table 10 and Fig. 11, it is observed that broadband characteristic is achieved for N = 5 mm.

Both from Table 11 and Fig. 12, it is noticed that broadband characteristic is achieved for W_g = 12 mm.

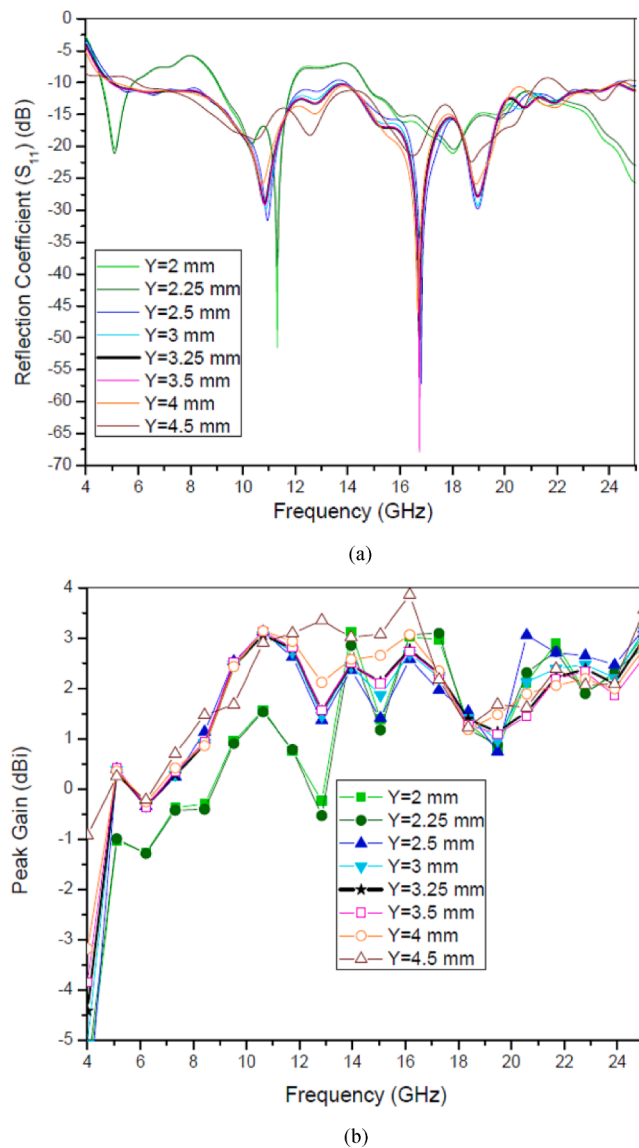


Fig. 7. (a) Reflection coefficient and (b) peak gain from Table 6.

Table 12 and Fig. 13 illustrate the effect of loading three step staircase structure ($J \times E, D \times H, C \times I$) in the feedline for better impedance matching. Broadband characteristics can be achieved when feed structure is optimized by modifying C, D, E, H, I and J. The optimum value of all the parameters and simulation results are summarized in Table 1 and Table 14.

5. Simulated and measured results

All the simulation results are attained by using CST Microwave Studio simulation software. The final model of the proposed antenna has been achieved by doing a detail parametric study as mentioned in Section 3.

Table 7

Variation of antenna characteristics with 'M' where $K = 6$ mm, $N = 5$ mm and $L = 2$ mm.

M (mm)	-10 dB impedance B.W. (GHz)	Peak Gain(dBi)	M (mm)	-10 dB impedance B.W. (GHz)	Peak Gain(dBi)
3	5.95–6.1, 6.77–11, 12.67–25	4.28	10.4	5–24.5	3.06
4	5.76–6.4, 6.9–13.78, 16–22.1,	3.19	11	6.24–19.47,	3.36
5	5.63–6.39, 7.3–12.8, 13.6–15.27, 16.6–18.5, 19.5–22.4,	3.34	11.5	6.43–11.53, 12.3–18.9,	3.30
5.5	5.55–6.35, 7.7–12.16, 13.13–15.4, 16.6–23.8	3.36	12	6.45–11.37, 12.9–13.9, 17.6–18.59	3.59

The simulation result of final design shows the broadband (5 GHz – 24.5 GHz) characteristics of the proposed antenna. The resonant frequencies are located at 10.8 GHz, 16.9 GHz and 18.84 GHz for the proposed antenna. The corresponding reflection coefficients are –28.5 dB, –52.8 dB, –26.5 dB respectively. Both the simulated and measured reflection coefficient and peak gain of proposed antenna are shown in Fig. 14 and Fig. 15 respectively. A measured peak gain of 3.06 dBi is obtained at 11.75 GHz frequency. Measured result is close to simulated result. The E plane simulated and measured co polarization and cross polarization radiation patterns are shown in Fig. 16(a), Fig. 17(a) and Fig. 18(a). The H plane simulated and measured co polarization and cross polarization radiation patterns are shown in Fig. 16(b), Fig. 17(b) and Fig. 18(b).

6. Design of proposed FSS integrated antenna

In the proposed work to obtain band stop response in the operating frequency range (5–24.5 GHz) a patch type FSS has been designed. This FSS acts as a partially reflecting surface. When the FSS is placed below the antenna at an optimum distance the back radiations of the antenna are reflected back by the FSS. When the reflected back radiation is in phase with the front radiation of the antenna, the resultant front radiation increases which leads to higher antenna gain. To design the unit cell of the proposed FSS, initially a square patch of side 8.8 mm is chosen as reference and then to get the required transmission coefficient for the entire bandwidth from 5 GHz to 24.5 GHz the modified patch length is taken as 8.6 mm and W_{FSS} as 8.8 mm. From the both end of the FSS unit cell along Y direction a slot of dimension 8.8 mm \times 0.1 mm is removed as shown in Fig. 19 to obtain the modified patch. Thereafter consecutive three circle shaped slots each of diameter 'P' are removed from modified patch. The distance between any two consecutive circles is 0.7 mm. All the parameter dimensions are given in Table 1. Theoretically the FSS structure consists of infinite number of unit cells placed periodically [21]. But in practical situation a dimension of 6×6 FSS is used to achieve compact size. The unit cell of FSS as well as 6×6 FSS is built on a FR4 substrate of 1.6 mm thickness with relative dielectric constant (ϵ_r) of 4.4, loss tangent ($\tan\delta$) of 0.02. The fabricated prototype of the 6×6 FSS and FSS integrated composite structure are illustrated in Fig. 20. Fig. 21 illustrates the pictorial representation of the combined structure of FSS and antenna. Here wave1 represents front wave radiated by antenna and wave2 represents reflected wave by the FSS.

Table 8

Variation of antenna characteristics with 'L' where $K = 6$ mm, $N = 5$ mm and $M = 10.4$ mm.

L (mm)	-10 dB impedance B.W. (GHz)	Peak Gain(dBi)	L (mm)	-10 dB impedance B.W. (GHz)	Peak Gain(dBi)
0.5	7.2–13.6, 15.8–22.6, 22.8–24.5	3.68	2	5–24.5	3.06
1	6.94–22.6, 23–23.5, 23.78–24.5	3.88	2.5	5.28–17.65, 18.2–21.5,	2.64
1.5	6.14–23.8, 24.36–24.7	3.49	3	5.42–11.66, 12.3–17.2, 19.3–20.9, 23.84–24.6	3.06
1.75	5.76–24,	3.09	3.5	5.55–11.4, 12.35–14.5, 15–16.97, 19.75–25	3.51

Table 9

Variation of antenna characteristics with 'K' where M = 10.4 mm, N = 5 mm and L = 2 mm.

K (mm)	-10 dB impedance B.W. (GHz)	Peak Gain(dBi)	K (mm)	-10 dB impedance B.W. (GHz)	Peak Gain (dBi)
1	11.3–13, 17.35–22.83, 23.7–25	3.74	5	8.5–13.5, 15–25,	3.16
2	11.2–13.4, 16.4–18, 19.7–22.6,	3.19	6	5–24.5	3.06
3	9.9–13.38, 16–17.9, 19.4–22.5,	2.99	7	4.6–19.26, 22.6–23.38,	3.13
4	8.93–13.38, 15.7–18, 18.9–22.45	3.23	8	4.65–12.12, 12.94–15, 22.56–23.57	4.03

Table 10

VARIATION OF ANTENNA CHARACTERISTICS WITH 'N' WHERE K = 6 mm, M = 10.4 mm and L = 2 mm.

N (mm)	-10 dB impedance B.W. (GHz)	Peak Gain(dBi)	N (mm)	-10 dB impedance B.W. (GHz)	Peak Gain (dBi)
0.5	8.68–14, 15.8–23.36	4.13	5	5–24.5	3.06
1.5	5.21–7.42, 9.2–10.4, 10.9–11.6, 12.6–13.3, 14–15.6	3.8	6	5.34–11.64, 13.66–17.43,	2.80
3	5.5–7.8, 9.4–10.7, 14–14.8	3.32	7	5.55–11.55, 13.6–17.5, 20.46–21.15,	3.28
4	5.8–8.9, 9.56–13.5, 18.5–20.4, 22.7–25	3.19	8	5.7–5.9, 8.72–10.46, 13.3–20.8, 22.94–25	3.4

Table 11

Variation of antenna characteristics with 'W_g' where K = 6 mm, M = 10.4 mm, N = 5 mm and L = 2 mm.

W _g (mm)	-10 dB impedance B.W. (GHz)	Peak Gain (dBi)	W _g (mm)	-10 dB impedance B.W. (GHz)	Peak Gain (dBi)
10.5	5.57–6.24, 8.5–21.4, 22.77–25	3.02	12.5	5–23.63,	3.31
11	5.6–7.7, 8.32–13.78, 14–21.7, 22.2–25	3.04	13	4.96–23.13	3.21
11.5	5.42–24.9	3.08	13.5	4.92–22.9,	2.64
12	5–24.5	3.06	14	4.81–13.6, 13.8–22.8	2.60

When FSS is placed at different distances from antenna (10 mm to 23 mm as indicated in Table 13) various changes in reflection coefficients are observed. When FSS is kept at 18 mm below the antenna, the reflection coefficient shows that the bandwidth of FSS integrated antenna is same as that of the original antenna as shown in Fig. 22. The peak gain of FSS integrated antenna for various position of FSS with respect to the antenna are shown in Fig. 23. Also it is observed from the Table 13 that the peak gain of the combined structure is maximized when the FSS is 18 mm below the antenna. The peak gain is increased from 3.06 dBi (Fig. 15) to 8.8 dBi (Fig. 23).

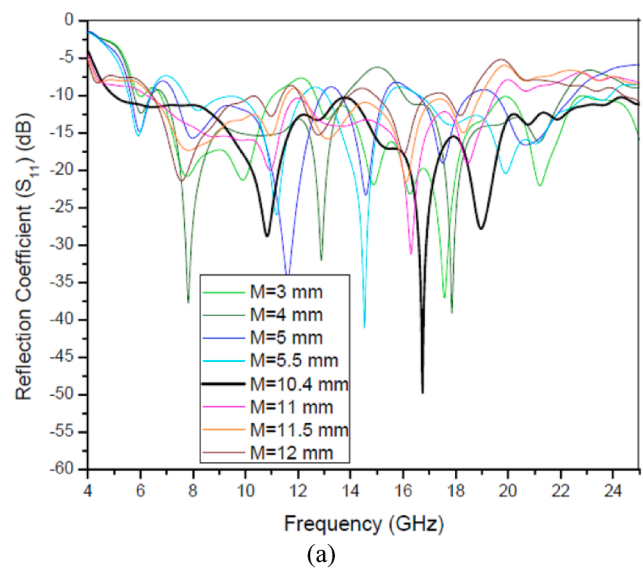
The simulated and measured transmission coefficient and reflection coefficient of proposed FSS are given in Fig. 24. Reflection phase of the proposed FSS is illustrated in Fig. 25.

The optimum distance between the FSS and antenna can be mathematically verified by calculating the far-field distance of the proposed antenna. Far-field distance of the antenna is $2D^2/\lambda$ where, D = largest dimension of antenna and λ = wavelength corresponding to the lowest frequency (5 GHz). $D^2 = 596 \text{ mm}^2$ and $\lambda = 60 \text{ mm}$ for the proposed antenna. Thus the far-field distance is 19.88 mm. The antenna height is 1.6 mm. So the optimum distance between antenna and FSS is kept at $19.88 \text{ mm} - 1.6 \text{ mm} = 18.28 \text{ mm} \approx 18 \text{ mm}$. From parametric studies (Table 13) it can be observed that the reflection characteristics of the antenna alter if the FSS is placed in the near-field region of the antenna. However in far-field region, there is no significant change in reflection characteristics for different positions of FSS. Thus, minimum distance of 18 mm is chosen for placement of FSS.

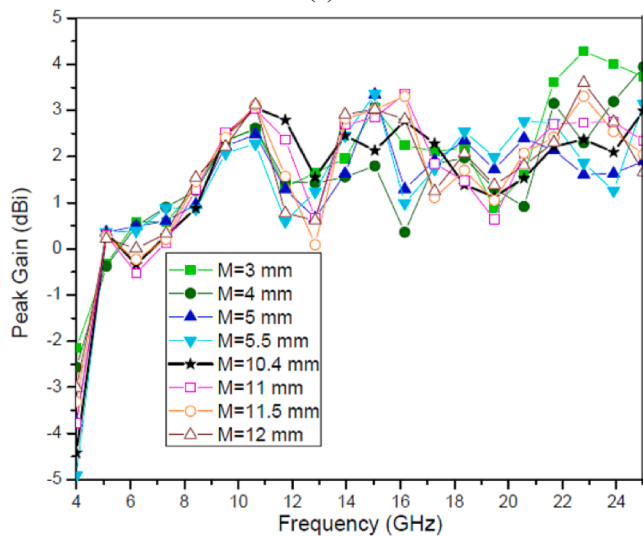
The FSS is used here as a reflector to enhance gain of antenna. The back waves radiated by antenna are reflected by FSS. If the reflected waves by FSS are in phase with the front waves of antenna then antenna gain is increased. The condition for which the reflected waves from FSS and the radiated waves from antenna to be in phase is given by equation (1)

$$\varphi_t = \varphi_{FSS} + 2\beta l \dots \quad (1)$$

Here φ_{FSS} is the reflection phase of the FSS, β is the propagation constant in free space and l is the distance between upper surface of the antenna and lower surface of the FSS, i.e., $l = h(\text{antenna}) + h_1(\text{gap}) + h(\text{FSS})$. $2\beta l$ is the roundtrip free space propagation phase delay between antenna and FSS. φ_t is the phase difference between the originally transmitted wave in front direction and back radiation reflected back by

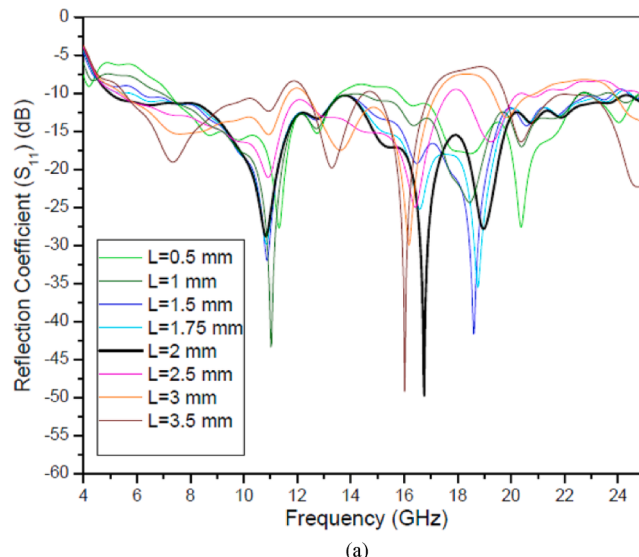


(a)

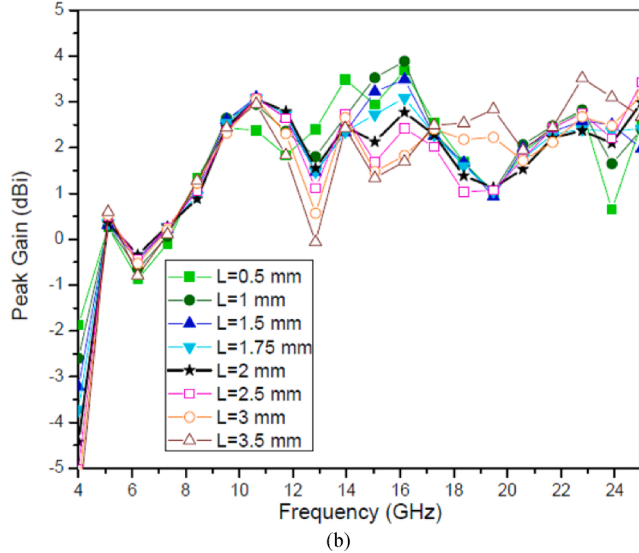


(b)

Fig. 8. (a) Reflection coefficient and (b) peak gain from Table 7.



(a)



(b)

Fig. 9. (a) Reflection coefficient and (b) peak gain from Table 8.

the FSS reflector at the point of original transmission in the front direction. For constructive phase coherence φ_t should be zero or an integral multiple of 2π . Dielectric constant (ϵ_r) of FR4 substrate is 4.4. So effective dielectric constant of the antenna and the FSS structure can be found by the Eq. (2).

$$\epsilon_{\text{effective}} = \frac{\epsilon_r + 1}{2} + \left(\frac{\epsilon_r - 1}{2} \right) \frac{1}{\sqrt{(1 + \frac{12h}{W})}} \quad (2)$$

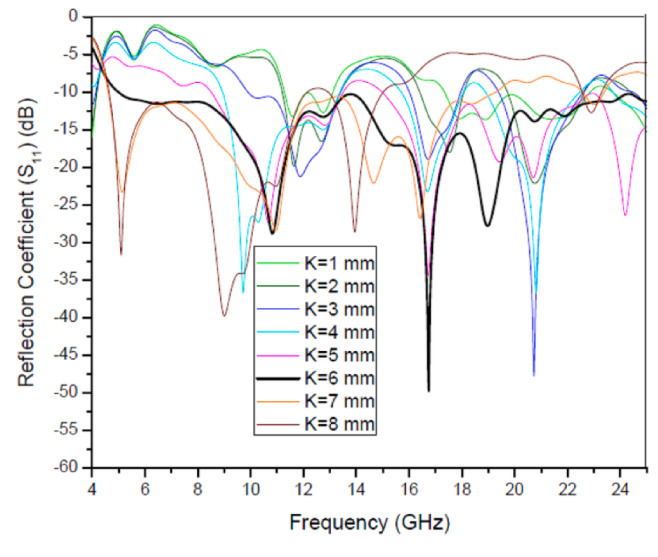
When $\frac{W}{h} \gg 1$ Where h is the antenna height or FSS height which is 1.6 mm and W is the antenna width or FSS width.

By putting all the values in (2) $\epsilon_{\text{effective}}(\text{Antenna}) = 3.8$ and $\epsilon_{\text{effective}}(\text{FSS}) = 3.65$ are obtained.

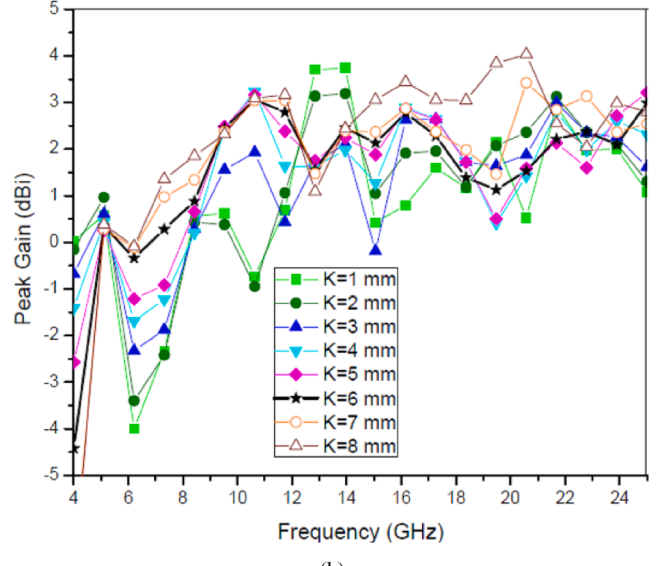
So cumulative effective dielectric constant between antenna and FSS can be found as

$$\epsilon_{\text{effective}}$$

$$= \frac{\epsilon_{\text{effective}}(\text{antenna}) \times h(\text{antenna}) + \epsilon_r(\text{air}) \times h_1(\text{gap}) + \epsilon_{\text{effective}}(\text{FSS}) \times h(\text{FSS})}{h(\text{antenna}) + h_1(\text{gap}) + h(\text{FSS})}$$



(a)



(b)

Fig. 10. (a) Reflection coefficient and (b) peak gain from Table 9.

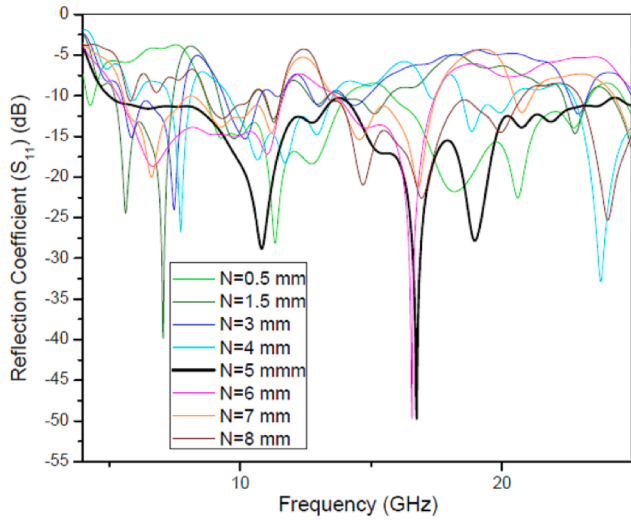
Putting all the values $\epsilon_{\text{effective}} = 1.41$ is obtained.. Now let us consider frequency 10.8 GHz as peak gain is obtained at this frequency. Wavelength (λ) corresponding to 10.8 GHz is 27.8 mm.

So effective wavelength can be found as $\lambda_{\text{eff}} = \frac{\lambda}{\sqrt{\epsilon_{\text{effective}}}} = 23.36$ mm.

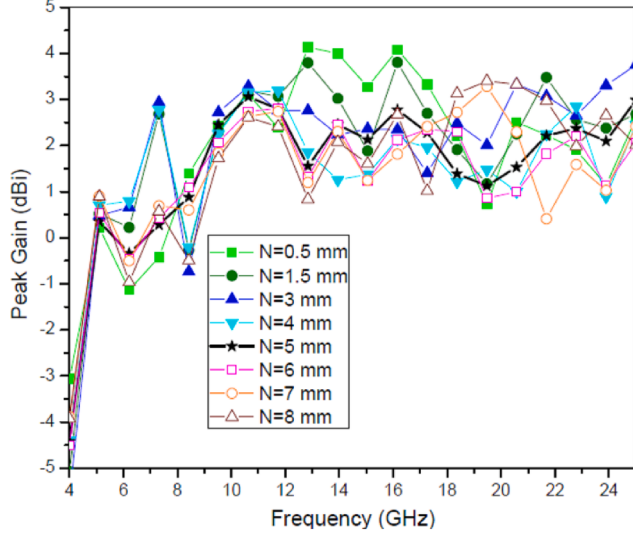
From Fig. 25 reflection phase φ_{FSS} is found to be 58 degree.

From Eq. (1) value of l can be found as $l = \frac{2n\pi - \varphi_{\text{FSS}}}{2\beta} \dots (3)$ [n = 0, 1, 2, 3....]

This condition is satisfied for many value of n. But a minimum distance of 18 mm in between antenna and FSS is needed. To satisfy this condition 'n' is taken as 2.Putting all the values in equation 3 we obtain the value of l as



(a)



(b)

Fig. 11. (a) Reflection coefficient and (b) peak gain from Table 10.

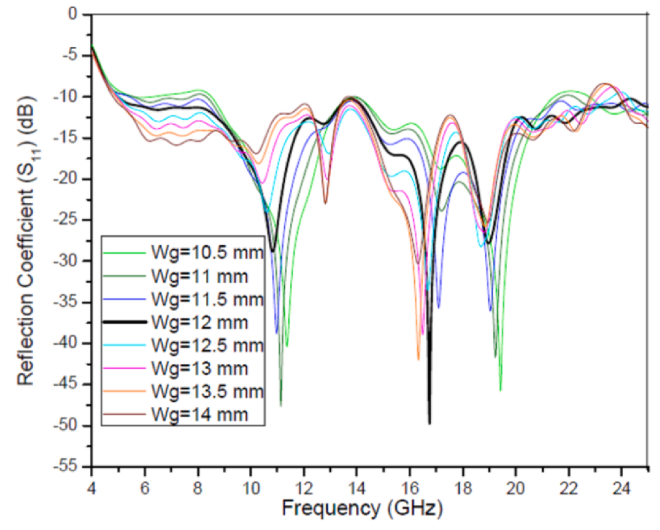
$$l = \frac{2n\pi - \varphi_{FSS}}{2\beta} = \frac{2n\pi - \varphi_{FSS}}{2\frac{2\pi}{\lambda_{eff}}} = \frac{2n\pi - \varphi_{FSS}}{4\pi} \times \lambda_{eff}$$

$$= \frac{(720 - 58)}{720} \times 23.36 = 21.47 \text{ mm}$$

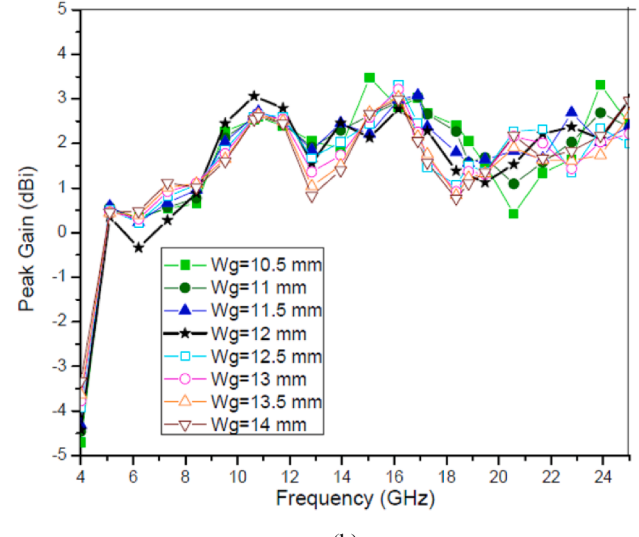
So the gap in between antenna and FSS is found to be $(21.47 \text{ mm} - 1.6 \text{ mm}) = 18.27 \text{ mm}$. Practically also maximum gain is obtained when FSS is placed 18 mm below the antenna.

Fig. 26 exhibits the peak gain of FSS mount antenna is 8.8 dBi at 10.8 GHz. The maximum gain enhancement of 5.9 dBi using FSS is obtained at 10.8 GHz (gain enhances from 2.9 dBi to 8.8 dBi).

Fig. 27 (a), 28 (a) and 29 (a) show the simulated and measured co-polarization and cross-polarization in E plane at 10.8 GHz, 16.9 GHz and 18.84 GHz with FSS respectively. Similarly H plane co-polarization and cross-polarization are shown in **Fig. 27(b)**, 28(b) and 29(b)



(a)



(b)

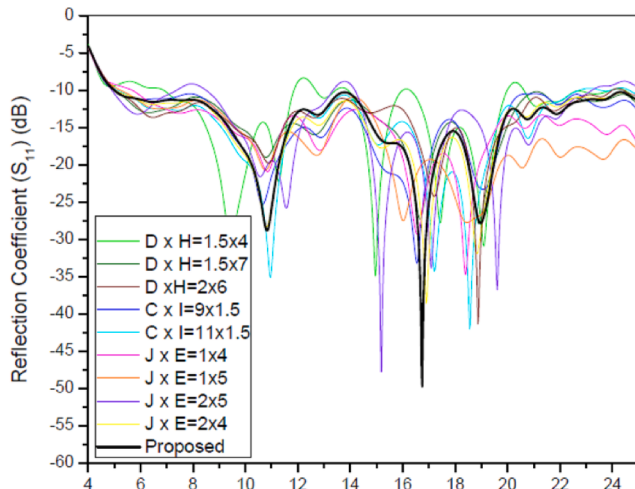
Fig. 12. (a) Reflection coefficient and (b) peak gain from Table 11.

respectively for the same resonant frequencies. Comparing the radiation pattern without FSS (**Figs. 16, 17, 18**) and with FSS (**Figs. 27, 28, 29**) it can be observed that introduction of FSS at suitable distance helps to achieve more directivity and high gain. Maximum isolation between co-polarized and cross-polarized waves are achieved as 10 dB, 10 dB and 12 dB for E-plane at the frequencies 10.8 GHz, 16.9 GHz and 18.84 GHz respectively for the antenna alone. Maximum isolation between co-polarized and cross-polarized waves are achieved as 21 dB, 20 dB and 20 dB for E-plane at the frequencies 10.8 GHz, 16.9 GHz and 18.84 GHz respectively for the FSS integrated antenna. Maximum isolation between co-polarized and cross-polarized waves is achieved as 8 dB, 12 dB and 17 dB for H-plane at the frequencies 10.8 GHz, 16.9 GHz and 18.84 GHz respectively for the antenna alone. Maximum isolation between co-polarized and cross-polarized waves are achieved as 20 dB, 20 dB and 15 dB for H-plane at the frequencies 10.8 GHz, 16.9 GHz and 18.84 GHz respectively for the FSS integrated antenna. Therefore the sufficient

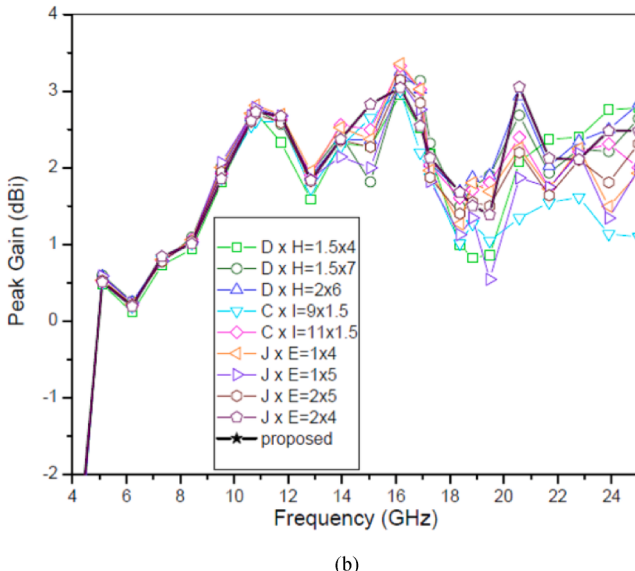
Table 12

Variation of antenna characteristics with 'y' where $F = 7.2$ mm, $G = 2.9$ mm and $x = 0.9$ mm.

$J \times E$ (mm^2)	-10 dB impedance B.W. (GHz)	Peak Gain (dBi)	$D \times H$ (mm^2)	-10 dB impedance B.W. (GHz)	Peak Gain (dBi)
1 × 4	5.67–25	3.23	1.5 × 4	7–11.8, 12.7–13.4, 14–16, 16.3–23.9	2.71
2 × 4	5–24.5	3.06	1.5 × 6	5–24.5	3.06
1 × 5	5.3–25	3.35	1.5 × 7	5.1–24.6	2.77
2 × 5	4.9–7.3, 8.5–13.3, 14.2–23.1	3.13	2 × 6	5.04–24.3	2.84
$C \times I$ (mm^2)	-10 dB impedance B.W. (GHz)	Peak Gain (dBi)	$C \times I$ (mm^2)	-10 dB impedance B.W. (GHz)	Peak Gain (dBi)
9 × 1.5	5.07–24	3.13	11 × 1.5	5.1–23.9	3
10 × 1.5	5–24.5	3.06			



(a)



(b)

Fig. 13. (a) Reflection coefficient and (b) peak gain from Table 12.

isolation between co-polarized wave and cross-polarized waves are achieved for FSS integrated antenna.

The simulated and measured results of impedance bandwidth and peak gain of the proposed antenna with FSS and without FSS are summarized in the Table 14.

The performance comparison in terms impedance bandwidth and peak gain obtained without FSS is presented in Table 15. It can also be concluded that the proposed antenna is very compact and exhibit

Table 13
The distance optimization between antenna and FSS.

Distance of FSS below the antenna (h_1)	-10 dB impedance bandwidth, GHz	Peak Gain, dBi
10 mm	8.4–13.7, 13.9–24.6	7.1
15 mm	6.2–6.6, 7.4–24.7	7.2
18 mm (proposed)	5–24.5	8.8
20 mm	4.71–24.8	7.5
23 mm	4.71–24.8	6.4

Table 14
Simulated and measured result summary of the proposed work.

Proposed work	-10 dB impedance Bandwidth (GHz)		Peak Gain, dBi	
	Simulated	Measured	Simulated	Measured
Antenna Without FSS	(5–24.5) GHz	(5.1–24.5) GHz	3.06 dBi at 10.63 GHz	3.06 dBi at 11.75 GHz
Antenna With FSS	(5–24.5) GHz	(5–24.6) GHz	8.68 dBi at 9.75 GHz	8.8 dBi at 10.8 GHz

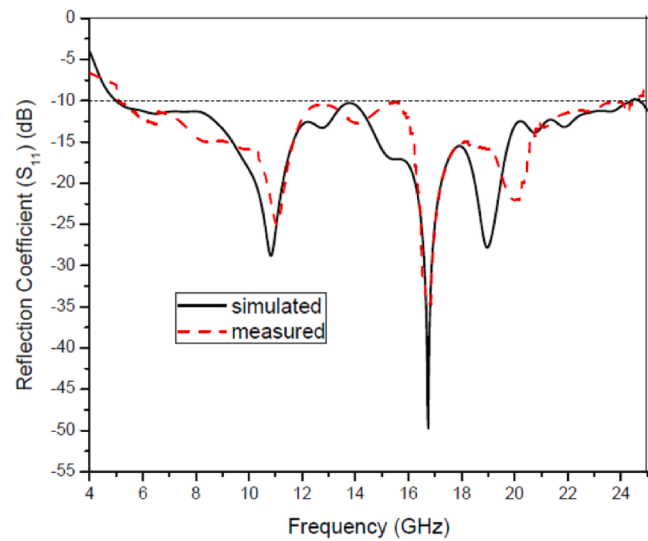


Fig. 14. Reflection coefficient.

broadband operation with moderate gain. Maximum gain enhancement of the FSS mount antenna is compared with the cited published literature presented in Table 16.

7. Conclusion

A compact broadband microstrip patch antenna with 'S' shaped

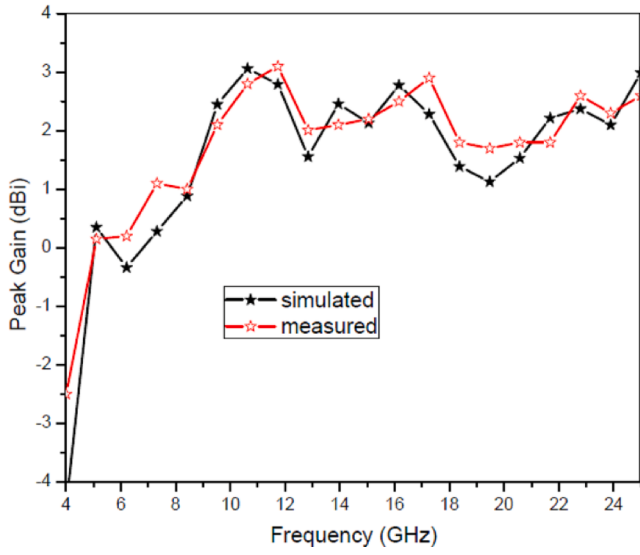


Fig. 15. Peak gain.

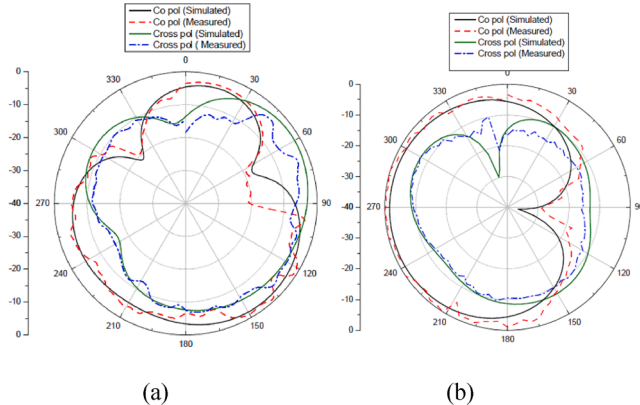


Fig. 16. (a) E field and (b) H field at 10.8 GHz.

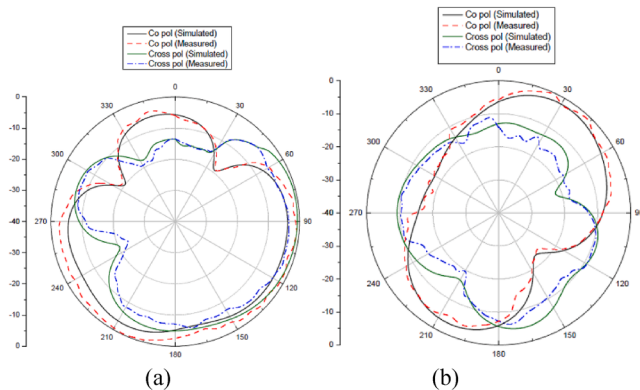


Fig. 17. (a) E field and (b) H field at 16.9 GHz.

patch, modified ground structure and modified feed structure is presented. The proposed antenna exhibits a large bandwidth of 19.5 GHz (5 GHz-24.5 GHz) having fractional bandwidth of 132% with a peak gain of 3.06 dBi. Antenna peak gain is further enhanced to 8.8 dBi for the same impedance bandwidth of the original antenna by placing a single-layer frequency selective surface (FSS) below the antenna at an optimum distance of 18 mm. Measured reflection coefficient, gain and radiation

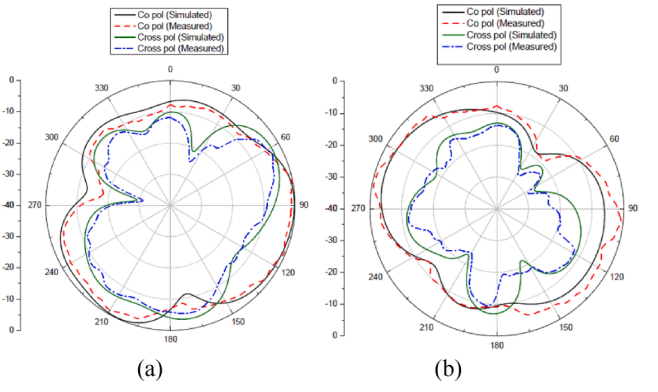


Fig. 18. (a) E field and (b) H field at 18.84 GHz.

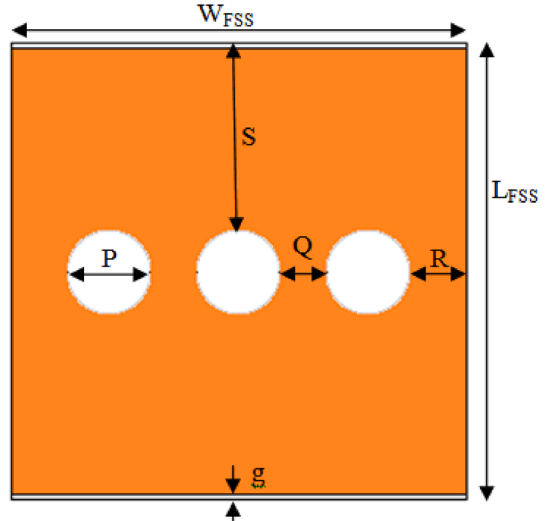


Fig. 19. Unit Cell of FSS.

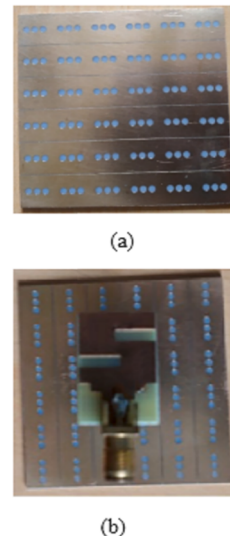


Fig. 20. Fabricated proto type (a) 6 × 6 FSS (b) composite structure.

pattern are very close to the simulation results. The overall dimension of FSS integrated antenna is 52.8 mm × 52.8 mm × 21.2 mm and can be used for UWB, X, Ku and K band applications. The proposed antenna without FSS can also be used in small handheld devices, wireless devices

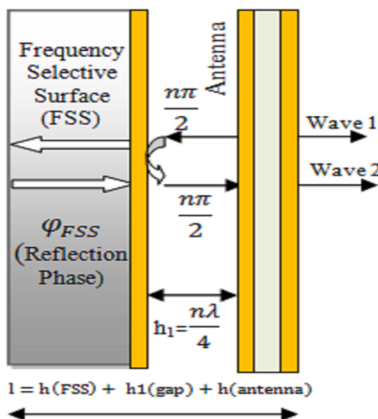


Fig. 21. Pictorial view of FSS integrated antenna.

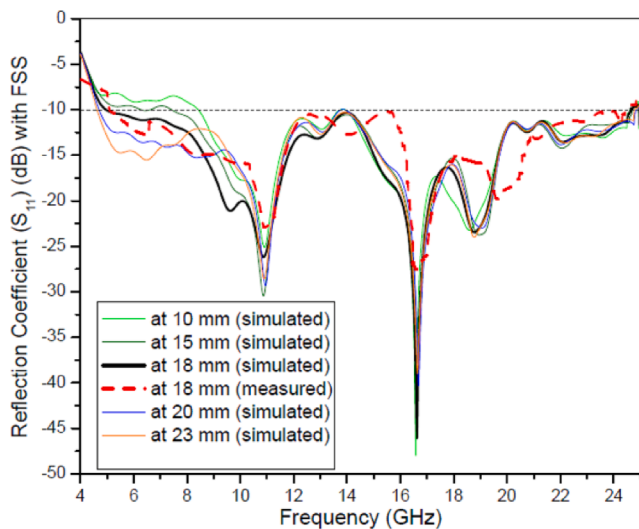
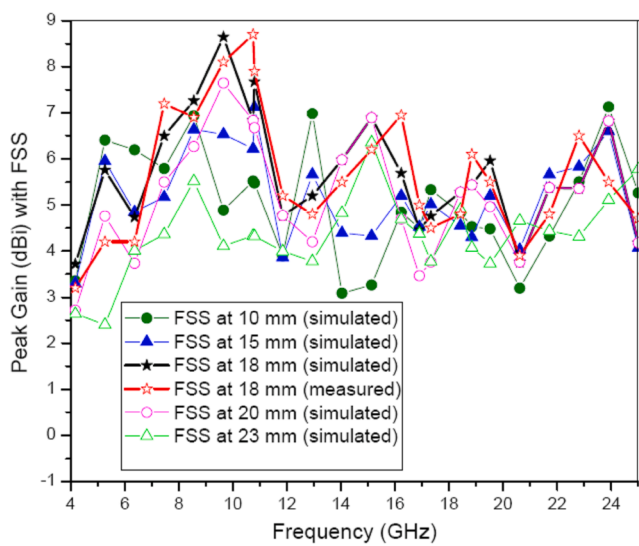
Fig. 22. Simulated and measured reflection coefficient (S_{11}) with FSS.

Fig. 23. Peak gain of the proposed FSS integrated antenna.

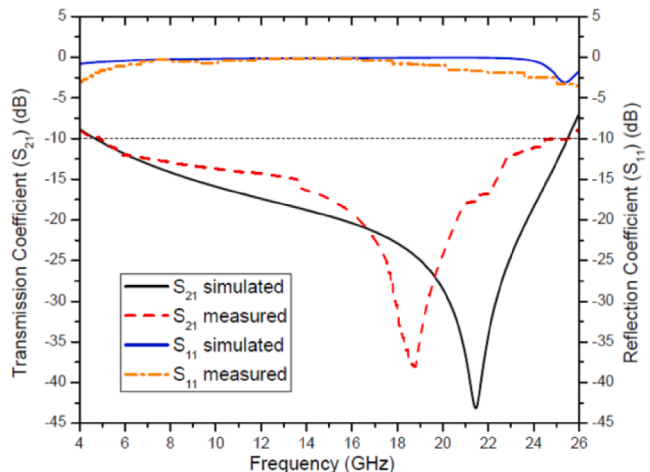


Fig. 24. Transmission/Reflection coefficient of proposed FSS.

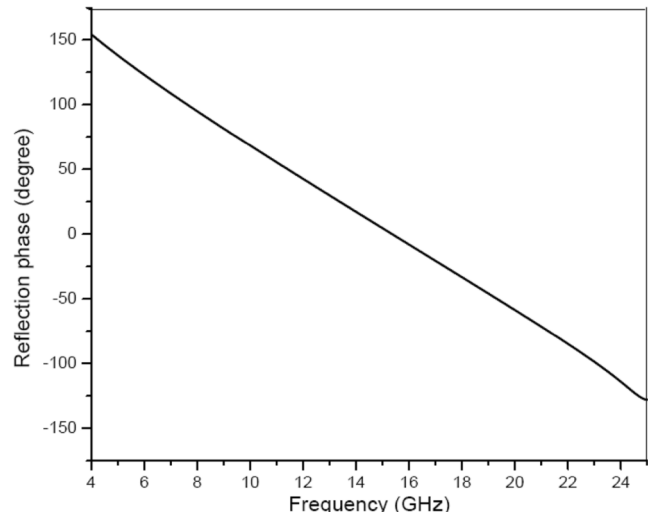


Fig. 25. Reflection phase of proposed FSS.

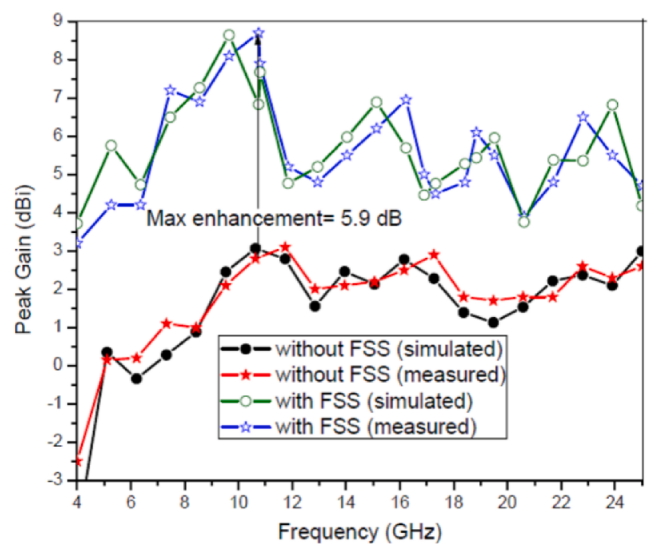


Fig. 26. Gain enhancement by using FSS at 18 mm distance below the antenna.

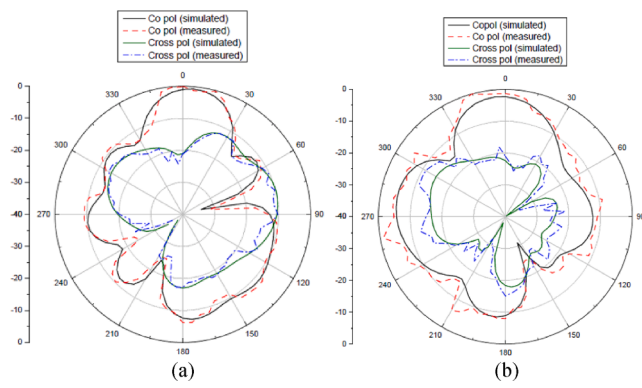


Fig. 27. (a) E field and (b) H field at 10.8 GHz with FSS.

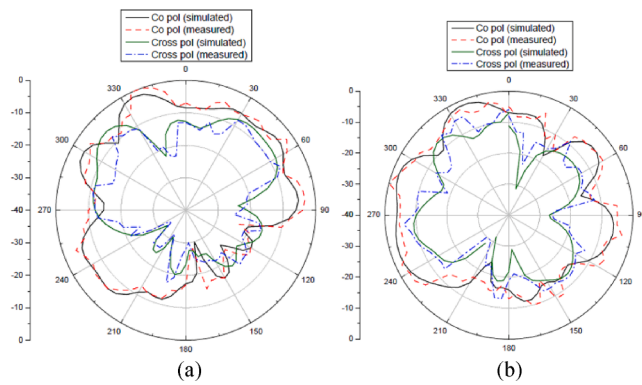


Fig. 28. (a) E field and (b) H field at 16.9 GHz with FSS.

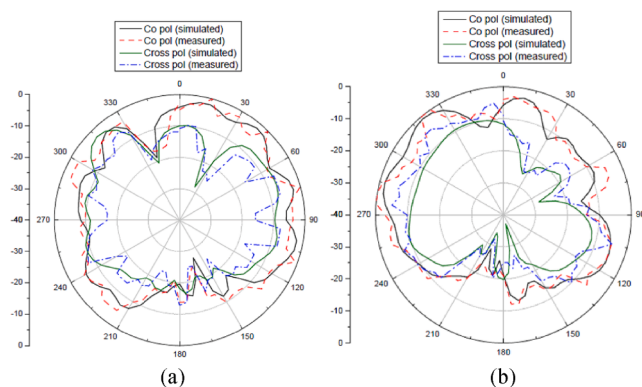


Fig. 29. (a) E field and (b) H field at 18.84 GHz with FSS.

Table 15
Comparison with the cited literature.

Ref. No	Antenna Dimensions (in mm ²)	B.W.(GHz)	Peak Gain (dBi)
[14]	35 × 30	3.05–13.4	4.5
[15]	45 × 36	3.6–12.6	5
[16]	25 × 25	3–12	6.5
[17]	20 × 27	4.7–14.9	4.2
[18]	16 × 22	3.1–18.6	4.1
[19]	26 × 26	3.05–11.9	6.3
Proposed	20 × 14	5–24.5	3.06

Table 16
Results of Proposed and Published Work.

Ref. No	Overall Dimensions using FSS	Maximum Gain (dBi) enhancement using FSS
[14]	44 × 44	4
[15]	86.5 × 86.5	7.5
[16]	135 × 135	2.5
[17]	84 x84	4.5
[18]	52 × 62.5	6.9
[19]	61 × 61	3.38
Proposed	52.8 × 52.8	5.9

and in satellites due to its very compact (20 mm × 14 mm × 1.6 mm) size.

Declaration of Competing Interest

The authors declare that they have no known competing financial interests or personal relationships that could have appeared to influence the work reported in this paper.

Acknowledgment

The authors would like to express a sincere appreciation and thankfulness to DETS, University of Kalyani, West Bengal, India, and Central Institute of Technology, Kokrajhar, BTAD Assam for providing great facilities such as IEEE Xplore digital library and research laboratory facility that made this research able to complete.

References

- Akinola S, Hashim I, Singh G. Gain and Bandwidth Enhancement Techniques of Microstrip Antenna: A Technical Review. 2019 International Conference on Computational Intelligence and Knowledge Economy (ICCIKE), December, 2019, Amity University Dubai, UAE.
- Patel JM, Patel SK, Thakkar FN. Analysis of W-slot loaded patch antenna for dualband operation. Int J Electron Commun (AEU), January, 2012;66(1):32–8.
- Liu Jianjun, Zhong Shunshi, Esselle Karu P. A printed elliptical monopole antenna with modified feeding structure for bandwidth enhancement. IEEE Trans Antennas Propag 2011;59(2):667–70.
- Ali S Abbas, Mohamed K Abdalazeez, Bandwidth Enhancement of Single Notch Planar UWB Antenna with Single Step Feed Line. 2015 IEEE Jordan Conference on Applied Electrical Engineering and Computing Technologies (AEECT).
- Shanmuganantham T, Raghavan S. Design of a compact broadband microstrip patch antenna with probe feeding for wireless applications. Int J Electron Commun (AEU). August, 2009;63(8):653–9.
- Alsaith MGN, Kanagasabai M. Compact UWB monopole antenna for automotive communications. IEEE Trans Antennas Propag. September, 2015;63(9):4204–8.
- Yibo Wang, Shuyu Wu, Jinju Zhang. Bandwidth enhanced miniaturized slot antenna on a thin microwave laminate. Int J Electron Commun (AEU) 2020;127: 153475. <https://doi.org/10.1016/j.aeue.2020.153475>.
- Nikolaou S, Abbasi MAB. Design of miniaturized super wideband printed monopole antenna operating from 0.7 to 18.5 GHz. Int J Electron Commun (AEU), August, 2020; vol. 123, Article 153273.
- Jafargholi Amir, Albarzadeh Seyed Abbas, Mazaheri Mohamad Hossein. wideband microstrip patch antenna using ENZ metamaterials. Microw Opt Technol Lett 2014; 56(9):2080–4.
- Pandey GK, Singh HS, Bharti PK, et al. UWB monopole antenna with enhanced gain and stable radiation pattern using gate like structures. Int Conf Microwave Photonics, ICMAP, Dhanbad, India, p. 4–7, December, 2013.
- Tang M-C, Shi T, Ziolkowski RW. Planar Ultrawideband Antennas With Improved Realized Gain Performance. IEEE Trans Antennas Propag. JANUARY 2016;vol. 64 (no. 1);p. 61–9.
- Yang D, Hu J, Sihao Liu. A Low Profile UWB Antenna for WBAN Applications. IEEE Access, May 2018;Vol. 6;p. 25214–9.
- Koziel Slawomir, Bekasiewicz Adrian. A structure and simulation-driven design of compact CPW-fed UWB antenna. IEEE Antennas Wirel Propag Lett 2016;15:750–3.
- Kundu S, Chatterjee A, Jana S, Parui SK. A Compact Umbrella-Shaped UWB Antenna with Gain Augmentation Using Frequency Selective Surface. Radioengineering. June 2018;vol. 27(no. 2);p. 484–54.
- Kushwaha Nagendra, Kumar Raj, Oli Tuhina. Design of a High-Gain Ultra-Wideband Slot Antenna using Frequency Selective Surface. Microw Opt Technol Letters 2014;56(6):1498–502.
- Parchin NO, Abd-Alhameed RA, Shen M. Gain Improvement of a UWB Antenna Using a Single-layer FSS. 2019 Photonics & Electromagnetics Research Symposium | Fall (PIERS | FALL), Xiamen, China, p. 1735–9, December 2019.

- [17] Das Priyanka, Mandal Kaushik. Modelling of ultra-wide stop band frequency selective surface to enhance the gain of a UWB antenna. *IET Microw Antennas Propag* 2019;13(3):269–77.
- [18] Mondal Rahul, Reddy P Soni, Sarkar Debasree Chanda, Sarkar Partha Pratim. Compact ultra-wideband antenna: improvement of gain and FBR across the entire bandwidth using FSS. *IET Microw Antennas Propag* 2020;14(1):66–74.
- [19] Al-Gburi AJA, Ibrahim IBM, Zeain MU, Zakaria Z. Compact Size and High Gain of CPW-Fed UWB Strawberry Artistic Shaped Printed Monopole Antennas Using FSS Single Layer Reflector. *IEEE Access*, May 2020;Vol. 8;p. 92697–707.
- [20] Balanis CA. *Antenna Theory, Analysis and Design*, Wiley.
- [21] Munk BA. *Frequency selective surfaces: theory and design*. New York: Wiley; 2000.